A Comparison of Time-Of-Flight MRA and Contrast-Enhanced MRA for Evaluating the Evolution of Intracranial Aneurysms

by
Siri Tantry

THESIS
Submitted in partial satisfaction of the requirements for degree of
MASTER OF SCIENCE

in

Biomedical Imaging

in the

GRADUATE DIVISION
of the
UNIVERSITY OF CALIFORNIA, SAN FRANCISCO

Approved:

DocuSigned by:
F1B602CAB7874F1...
David Saloner
Chair

DocuSigned by:
Alastair Martin
Alastair Martin

DocuSigned by:
Kambiz Nael
Kambiz Nael

DocuSigned by:
Dimitrios Mitsouras
95668F65C7D24FE...
Dimitrios Mitsouras

Committee Members

Acknowledgements

First of all, I would like to sincerely thank Dr. David Saloner, my thesis advisor, for the immense support, guidance, and mentorship that shaped me into the student I am today. Sitting with me and teaching me the basics of the research I was doing, as well as showing me the big picture of the questions we were asking, showed me how significance is found in every single question.

To my thesis committee - Dr. Alastair Martin, Dr. Kambiz Nael, and Dr. Dimitrios Mitsouras - thank you for your guidance and input regarding my thesis. Every suggestion and idea that was provided truly enhanced my scientific inquiry and encouraged me to think more deeply about the analysis I was doing.

I would also like to thank the Vascular Research team, specifically Evan Kao and Alexandra Gill, for their immense support and contributions to my thesis. Whether it was supporting me throughout the data collection or answering my numerous questions about the analysis pipeline, I am truly grateful for their help.

Last but certainly not least, I would like to thank my family and friends who supported me throughout my thesis. All of this would not have been possible without the support of my parents and my sister, who encouraged me to dream big and do my best. Without their constant support in all aspects of my life, I would not have been able to do any of this. A special mention to my friends who gave me the space to talk about my work and acted as my audience and sounding board throughout my thesis preparations.

With my sincerest and deepest regards, **thank you all for everything**.

Siri Venkatesh Tantry

A Comparison of Time-Of-Flight MRA and Contrast-Enhanced MRA for Evaluating the Evolution of Intracranial Aneurysm

Siri Tantry

Abstract

Determination of changes in the volume of a cerebral aneurysm over time is important as increased growth rates are indicators of elevated rupture risk. Two major magnetic resonance (MR) angiographic options are available for defining the contours of cerebral aneurysms: time-of-flight (TOF) MRA and Contrast-Enhanced (CE) MRA. Past work aimed to assess the reliability of contrast-enhanced MRA in monitoring serial volumetric changes of unruptured intracranial aneurysms but less has been reported for TOF methods. The relative performance of these two methods is poorly established. In the past, comparisons between the two techniques have used single time point patient data. In this project, we used patient data from multiple time points to compare and evaluate the degree of reproducibility between TOF-MRA and CE-MRA using co-registration techniques to see which method has better consistency. Using a standardized protocol for non-invasive MRI, specifically TOF and CE, a preliminary sample size of 9 aneurysms was analyzed through the co-registration and segmentation pipeline. Results showed that 61.5% of the TOF-MRA imaging data and 23.1% of the CE-MRA imaging scans were invalid to meaningfully analyze the aneurysm volume changes. Additionally, it was consistently shown that TOF-MRA had magnetization saturation effects that were more pronounced with increasing aneurysm size and volumes at the first timepoint were consistently reported lower than their CE-MRA counterparts. Thus, while TOF-MRA seems to work reliably in aneurysms that are less than 6 mm in size, it fails to reliably work on aneurysms larger than 6 mm. Future directions will focus on increasing the sample size with the aim of obtaining the TOF-MRA coefficient of variance; the potential of adding smoothing for the TOF-MRA image processing should also be assessed. In short, based on preliminary data analysis, TOF-MRA has many image quality problems affecting the reliability and validity of its aneurysm volumetric analysis.

Table of Contents

List of Figures

List of Tables

Introduction

The prevalence of unruptured intracranial aneurysms is estimated to be 3.2% in the adult population. With increased availability of neuroimaging, there has been an increased frequency in detection of intracranial aneurysms. During follow-up aneurysms may: remain asymptomatic and stable; show a systematic increase in the aneurysm dimension; or a rupture may occur due to the increase in the aneurysm size. Annual rupture risk depends on the size, shape, and location of the aneurysm and ranges from 2% to 10% (van der Kamp et al, 2021). Thus, determining whether the aneurysm is stable or growing over time is of high importance for assessing the rupture risk. Moreover, because rupture location can affect patient outcome, monitoring the risk becomes further imperative. Because intracranial aneurysms can have irregular and complicated geometry presentation, reproducible and accurate measurements of the aneurysm diameter is difficult. Thus, past work using contrast-enhanced MRA (CE-MRA) considered monitoring serial volumetric changes of unruptured intracranial aneurysms. Using a fully automated pipeline that took account of sources of error such as timing delay, they found that the coefficient of variance was 5.5% of the aneurysm volume (Liu et al, 2021), the relative growth rate was dependent on the location and were able to conclude that the volume measurement of unruptured intracranial aneurysms by CE-MRA was a reliable metric for tracking aneurysm growth.

Between the two imaging techniques, CE-MRA and time-of-flight MRA (TOF-MRA), it has been found that for the evaluation and visualization of intracranial aneurysms, CE-MRA is generally superior to TOF-MRA (Cirillo et al, 2013).

CE-MRA offers better visualization of the aneurysm neck, sac shape, and adjacent vessel branches. Yet, TOF-MRA is more routinely used in the clinical setting because it is non-invasive (requiring no contrast) and has higher resolution compared to CE-MRA. Furthermore, it does not require any complicated timing considerations, which are inherent to CE-MRA. However, TOF-MRA scans

suffer from flow-related artifacts and overestimation of stenosis, which may affect the reproducibility and reliability of using TOF-MRA data to monitor serial aneurysm volumetric changes.

Having a reliable metric of evaluation for aneurysmal changes would help understand important features related to the trajectory of the aneurysm growth. For example, some aneurysm cases show a linear and continuous growth pattern, whereas others show periods of relative stability followed by periods of intermittent rapid growth. These differences in growth patterns could imply different pathological processes, which would require different clinical management of the aneurysm.

This project aims to compare the reproducibility of volumetric measurement by TOF-MRA with CE-MRA to understand which method offers better consistency as a means of establishing a criterion for likely growth of aneurysms and further identify variables predictive of growth. Additionally, this project aims to understand the size threshold for aneurysms in which TOF-MRA volumetric analysis has similar reliability with CE-MRA volumetric analysis.

Materials and Methods

Patient Population

This retrospective study was conducted under institutional review board approval of the UCSF Medical Center. All subjects gave written informed consent for study participation. While the study has since shifted from the original study design to become a part of the clinical routine, the original study design noted a recruitment of 121 subjects. Of these subjects, 79 subjects with saccular intracranial aneurysms were recruited over a period of three years with a target recruitment of 26 patients per year, and an additional 20 subjects with giant fusiform aneurysms were recruited. Once this target was reached, enrollment was expanded to 150 subjects.

The broad inclusion criteria from the original study included participants between the ages of 18 years and 100 years as well as those who were known to have intracranial aneurysms that were not

scheduled for surgical or endovascular treatment. For this study, subjects could have had saccular or fusiform aneurysms of the intracranial vessels.

CE-MRA and TOF-MRA Protocol

Progression over time in the aneurysm lumen volume and/or volume of intralumenal thrombus is measured from co-registered serial imaging studies.

All the subjects were imaged using high-resolution contrast-enhanced 3D Magnetic Resonance Angiography and 3D balanced steady-state imaging. In addition, magnetic Resonance Velocimetry was performed to measure flow velocities in the parent vessels of the aneurysms. Subjects were asked to return for follow-up imaging at 6-month intervals, and imaging studies from each time point are co-registered to determine aneurysm growth locations.

Specific scan parameters for the CE-MRA image acquisition at 3T included: TR/TE = 3.7/1.4 ms, flip angle = 20°, slice thickness = 0.7 mm, NEX = 1, pixel bandwidth = 504 Hz/pixel, in-plane resolution = 0.7 mm x 0.7 mm, total acquisition time = 30sec, slab thickness = 84 mm.

For CE-MRA, first, a timing bolus must be calculated to assess how long the contrast takes to enter the vessel of interest. Once this timing is calculated and obtained, the actual acquisition of the images is timed based on the bolus. Thus, if the timing is delayed or early, it can lead to timing image artifacts in the CE-MRA scans.

Specific scan parameters for the TOF-MRA image acquisition at 3T included: TR/TE = 43.9/3.7 ms, flip angle = 22°, slice thickness = 0.5 mm, NEX = 1, pixel bandwidth = 187 Hz/pixel, in-plane resolution = 0.5mm x0.5 mm, total acquisition time = 84.54 sec, slab thickness = 84.5 mm.

Clinical Data Collection Process

The collection of the clinical data for the analysis to be done started with using a combination of string searches through mPower and AIR that included the words AGES and aneurysm to obtain all

clinical subjects that had these words included in the clinical notes. With this, individual clinical notes were assessed to confirm the presence of untreated aneurysm that were larger than 2.5 mm. With many clinical notes noting presence of treated aneurysms and noting uncertainty of an aneurysm present compared to an infundibulum, possible subjects to analyze went from 134 to 56. After manually checking the clinical scans to ensure that the scans were done in UCSF on the same scanner and all timepoints had both TOF-MRA and CE-MRA scans, the sample size reduced to 22.

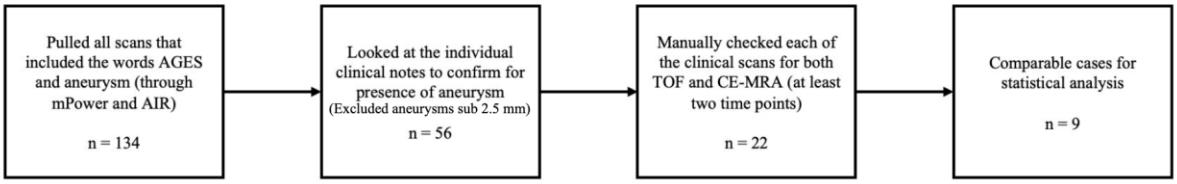

Figure 1. Summary of Clinical Data Collection
A diagram summarizing the clinical data collection and the sample sizes as each criterion or stage was implemented

Longitudinal Analysis of the Aneurysm Volume

Aneurysm volume analysis was performed using two thresholding iterations and were selected using the same windowing techniques as in clinical practice to maximize luminal volume while excluding extraluminal regions. This selection was repeated on all consecutive datasets, and 3D volumes were placed into spatial co-registration. The second thresholding step was performed using a reference length of vessel that was presumed to have a constant volume during all the serial time points. The reference vessel identification varied depending on the aneurysm location, but generally was located near the aneurysm on the same artery.

The processing pipeline included exporting DICOM images in the Visualization ToolKit format. Isosurfaces for baseline and follow-up studies were imported into the 3D modeling software Geomagic Design X (3D Systems) and were co-registered using a manually picked, landmark-based registration (Figure 2). Until volume matching was achieved for the reference length, the threshold was adjusted, and

a new isosurface was generated. The cut planes were then prescribed transverse to the arteries at the proximal and distal ends of the aneurysmal segment, and the volume contained within the isosurfaces between those planes was calculated (Figure 3).

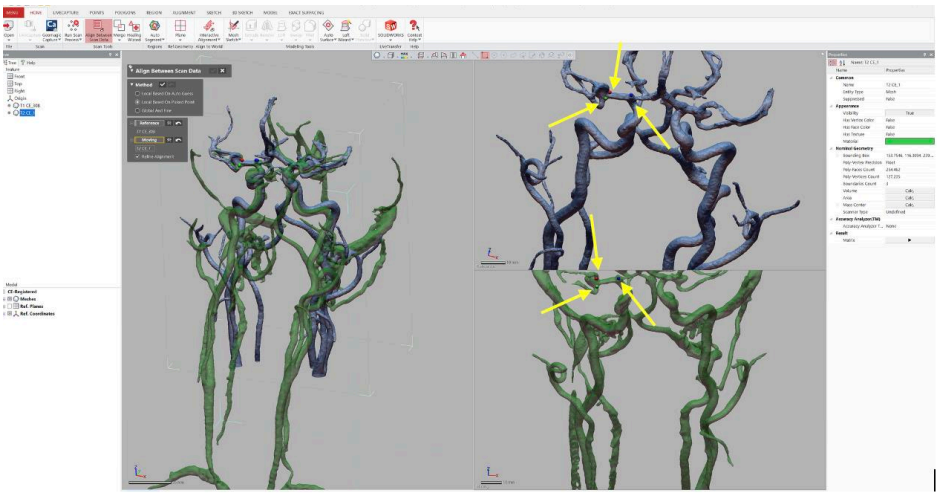

Figure 2. Landmark-Based Registration
A screenshot of the manual landmark-based registration step from the pipeline. The top slice on the right side is the first time-point scan of a left middle cerebral artery (MCA) aneurysm, and the bottom slice is a surface rendering of the same aneurysm but at the second time-point. The yellow arrows show the three locations where the landmark registration was done between the two time points.

Figure 3. Volume Analysis
A screenshot of the same left middle cerebral artery (MCA) aneurysm visualized in Figure 2, showing the cut planes step from the pipeline, which is used to calculate the volume of the aneurysm that is contained within the isosurfaces.

Inclusion and Exclusion Criteria

The aneurysm images that were included specifically for this study had to meet the criteria that the patient was imaged on a UCSF MR scanner with the appropriate protocol, including TOF-MRA and CE-MRA, and the aneurysms needed to have at least two time points that could be co-registered.

Patients who did not have a minimum of two time points for both Contrast-Enhanced and Time-of-Flight, or were not scanned on a UCSF scanner, or whose MRA images had technical problems such as having the aneurysm cut off in the image, were excluded from the analysis for this project.

Patients that had aneurysms smaller than 2.5 mm and patients that had treated aneurysms (for example coiled aneurysms) were also excluded from the study.

Results

Comparisons using the pipeline were performed on a total of 22 aneurysms. Using data for comparison of the reliability of Time-of-Flight measurements with Contrast-Enhanced, some scans had to be excluded from the statistical analysis due to image quality effects, resulting in a total of 9 scans that could be considered when performing statistical analysis (Table 1). For the purposes of our study comparing how reliable TOF-MRA was against CE-MRA, adding an additional layer of including thrombus cases (Figure 5, 6, and 7) was not explored, but is a future direction once more aneurysm samples are analyzed. Because the sample size is small, a meaningful statistical analysis is not yet possible but is a future direction as more aneurysm samples are analyzed. A power analysis showed that in this subset, CE-MRA's growth signal was strong and adequately powered to detect with confidence. TOF-MRA's growth signal, however, would require a larger sample of at least 22 subjects to confirm statistically.

Table 1: Image Quality Summary
Summary of the image quality that affected the volumetric analysis of the aneurysm (if present) leading to Exclusions.

Category	Count	% of Total (n=22)	% of Exclusions (n=13)
Included — comparable TOF & CE	9	40.9%	—
Contour Failure — TOF saturation effect	8	36.4%	61.5%
Contour Failure — CE scan quality issue	3	13.6%	23.1%
Lumen Contour Failure— aneurysm thrombus affecting output	2	9.1%	15.4%
Total Analysis Failure (all reasons)	13	59.1%	100%
Total scans	22	100%	—

Visual comparisons (Figure 4) between the TOF-MRA and CE-MRA further confirmed that TOF-MRA image quality was often poor compared to CE-MRA in relation to volumetric analysis, which can be seen to result from the saturation of signal in regions of slowly recirculating blood (referred to as saturation effects in Table 1) in the TOF-MRA. Of the 22 cases where the aneurysm was greater than 3mm and where baseline and follow-up time points were available, 41% were amenable to systematic

analysis, 45% were not analyzable because of TOF-MRA effects, and the remaining 14% were not analyzable because of CE-MRA effects.

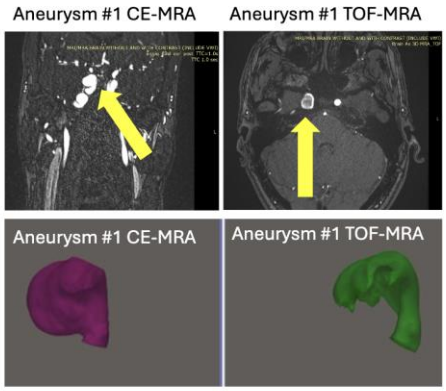

Figure 4. Aneurysm #1
Aneurysm #1 showing that TOF (right) has incomplete filling of the aneurysm in contrast to the CE-MRA (left) where there is filling.

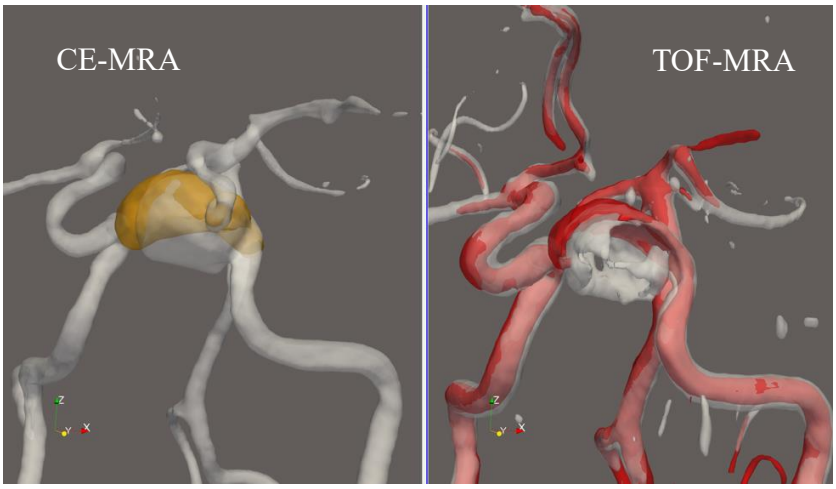

Figure 5. Aneurysm #4
Surface rendering of Aneurysm #4 that shows the presence of thrombus and incomplete TOF vessel signal saturation (right) for Aneurysm #4.

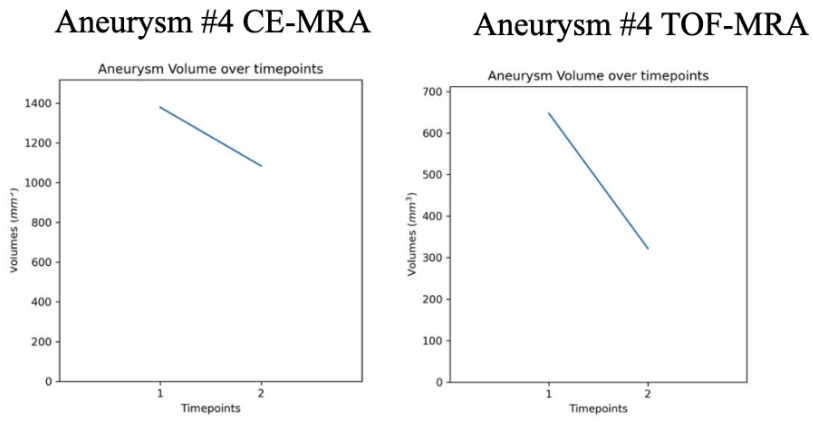

Figure 6. Aneurysm #4 Volumetric Analysis
Volumetric Analysis of Aneurysm #4 TOF-MRA and CE-MRA showing a decrease in volume due to thrombus and the compounded effect of incomplete signal filling present in TOF-MRA.

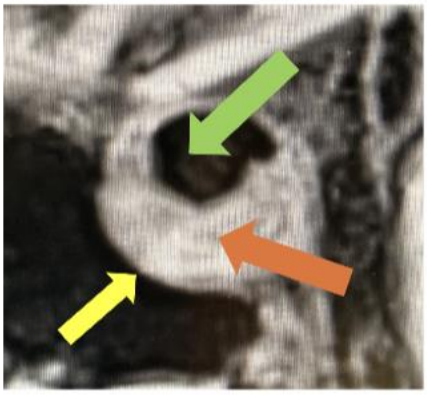

Figure 7. Black Blood Imaging of Aneurysm #4
Native Image of Aneurysm #4 via Black Blood Imaging Scan showing the presence of thrombus for the aneurysm at timepoint #2. The yellow arrow is pointing to the outer wall, the orange arrow is pointing to the thrombus, and the green arrow is pointing to the lumen of the aneurysm.

For some TOF image quality cases that originally needed to be excluded due to the automated pipeline being unable to match thresholding values between time points, the scans were salvageable through manual segmentation and cleaning of the scan to do volumetric analysis of the aneurysm (Figure 8). However, we did not include the cleaned-up scans as we were comparing the reliability of the modalities through the automated pipeline. It must also be noted that in such cases where the automated pipeline failed on the TOF-MRA modality, the aneurysm volume started off at close to 0 mm^3 which when compared to the CE-MRA surface rendering indicated clear unreliability (Figure 9 and 10).

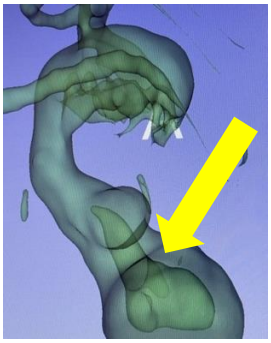

Figure 8. TOF-MRA Scan Quality Artifact
3D Surface Rendering of poor image quality leading to internal TOF artifact in aneurysm leading to inaccurate volumetric analysis which needed to be manually removed and cleaned.

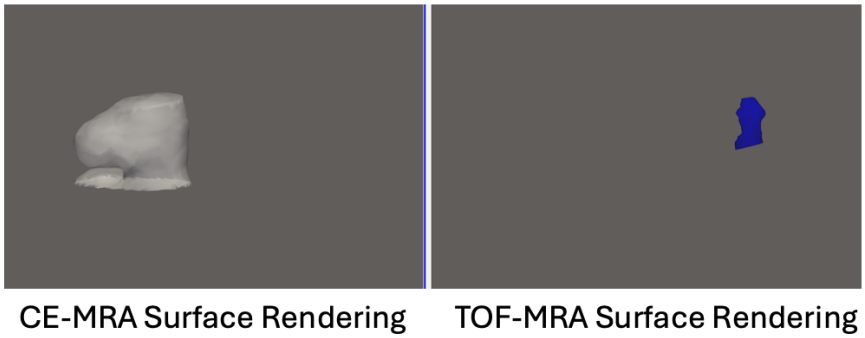

Figure 9. Thresholding Trade-off Visual Representation
Visual representation of the tradeoff between removing noise in the TOF-MRA (on the right) leading to reduced size in Aneurysm #2 based on the original (unedited) scans. The accurate-size representation of Aneurysm #2 is visualized through CE-MRA (left).

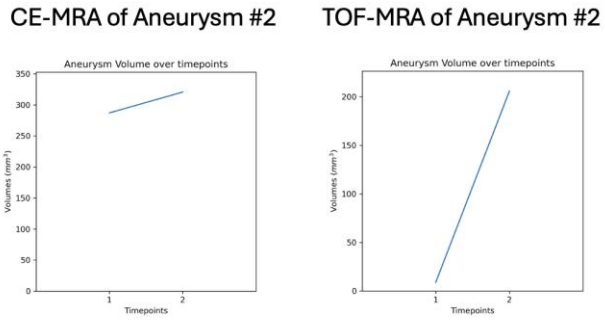

Figure 10. Volumetric Analysis of Aneurysm #2
TOF-MRA (right) aneurysm volume starting off close to 0 mm^3 which is inaccurate, due to the thresholding and volume tradeoff caused by the TOF-MRA image quality artifact. This volumetric analysis can be contrasted with CE-MRA (left) of the same Aneurysm #2.

In the CE-MRA of one of the aneurysms it was difficult to accurately define the contours of the aneurysm relative to the adjacent signal in the cavernous carotid sinus. This created an appearance of the presence of noise and the existence of a vessel imaging artifact (Figure 11) due to inaccurate timing delay causing a lack of separation between the arterial and venous signal and resulting in ineffective aneurysm isolation. The presence of the artifact causes the aneurysm volume between the first timepoint and second timepoint to be inaccurately represented as a decrease in the volume for CE-MRA, which was not reflected to the same degree in the volumetric analysis of the TOF-MRA (Figure 12).

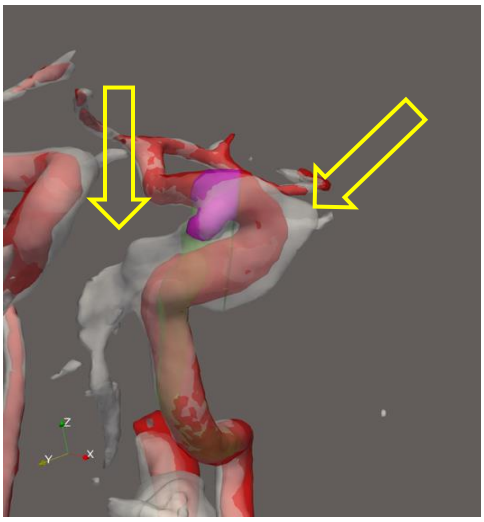

Figure 11. CE-MRA Timing Artifact
Presence of artifact surrounding the vessel for CE-MRA for Aneurysm #6.

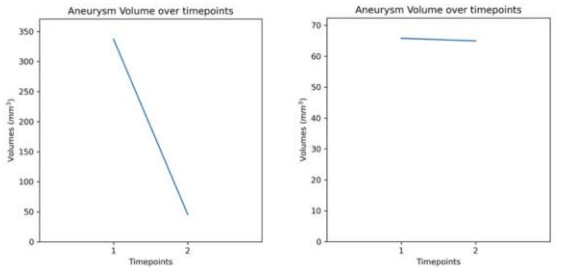

Aneurysm #6 CE-MRA Aneurysm #6 TOF-MRA

Figure 12. Volumetric Analysis of Aneurysm #6
CE-MRA (left) volumetric analysis inaccurately showing a decrease in the aneurysm volume for Aneurysm #6 in contrast with TOF-MRA (right) which does not reflect the same magnitude of decrease in volume for the same aneurysm.

For the cases in which the automated pipeline worked on both TOF-MRA and CE-MRA, checking the selected thresholding and overlaying them with the native images showed that the selective thresholding done by the pipeline accurately captured the aneurysm (Figure 13). Specifically, the pipeline used mathematical optimization bounded to an intensity precision floor of 0.01 grayscale units and a physical shape-reconstruction tolerance of 0.001 spatial units along the vessel axis.

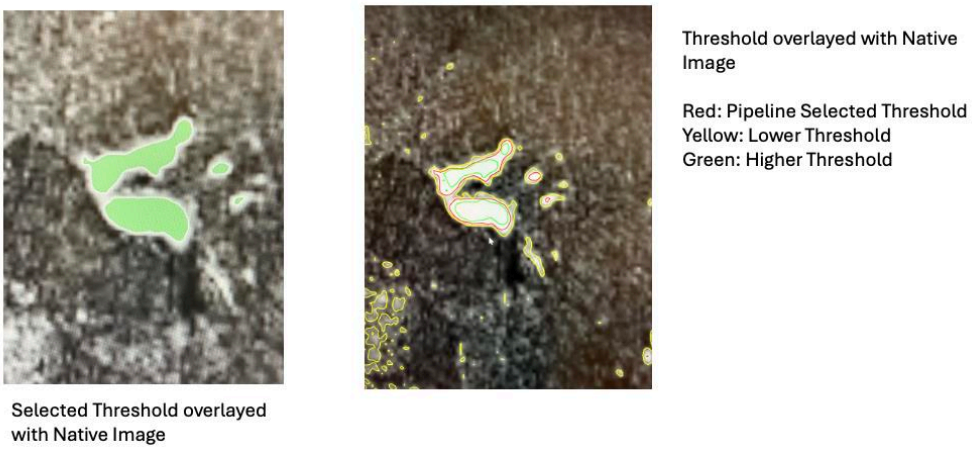

Figure 13. Thresholding Overlay
Aneurysm #22 Thresholding Overlay

The different aneurysms were ordered by size to explore the size threshold at which using TOF-MRA for volumetric analysis was reliable and consistent with CE-MRA. In instances where the aneurysm was less than 6 mm and there was no pronounced saturation of signal in regions of slowly recirculating blood, the TOF-MRA followed a similar trend to the CE-MRA volumetric analysis graphs, indicating either a slight increase or the same volume over the time points. For aneurysms that were greater than 6 mm, the TOF-MRA graph consistently showed a decrease over time points, which was not reflected in the CE-MRA analysis, indicating trend and volumetric analysis discrepancies between the two modalities.

Of the cases that had comparable quality of TOF and CE-MRA, statistical analysis was performed (Table 2) and the Pearson correlation of agreement of the aneurysm volume between TOF and CE-MRA was 0.935 for Timepoint 1 and 0.919 for Timepoint 2. However, this strong agreement between the two

modalities is lost when looking at the agreement on growth as the Pearson correlation drops to 0.344 (Figure 14).

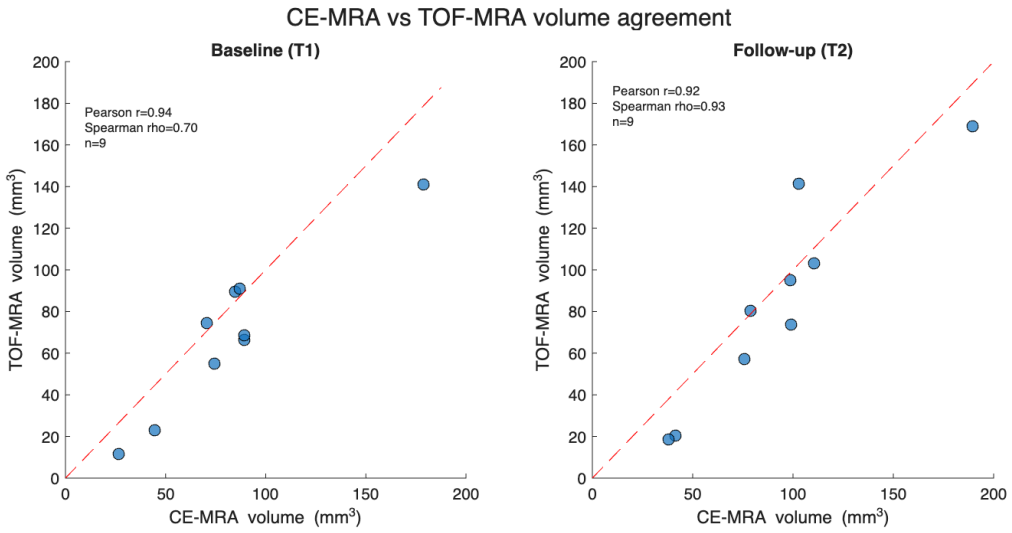

Figure 14. Correlation of Agreement
Correlation of Agreement between TOF and CE for Timepoint 1 (Baseline) and Timepoint 2 (Follow-up). Baseline shows to have a Pearson r coefficient of 0.94, and the Follow-up shows to have a Pearson r coefficient of 0.92.

This finding is further reinforced by the ICC Agreement values that compared CE with TOF in which Timepoint 1 had an ICC value of 0.886, Timepoint 2 had a value of 0.907, and the growth ICC value was 0.207. When looking at the Bland-Altman Bias Analysis (Figure 15), Timepoint 1 had a bias of 13.9 mm^3, Timepoint 2 had a bias of 8.5 mm^3, and the Growth had a bias of -5.3 mm^3, with the Limits of Agreement spanning around 88.1 mm^3, indicative that the TOF-MRA systematically underestimates volume when compared to CE.

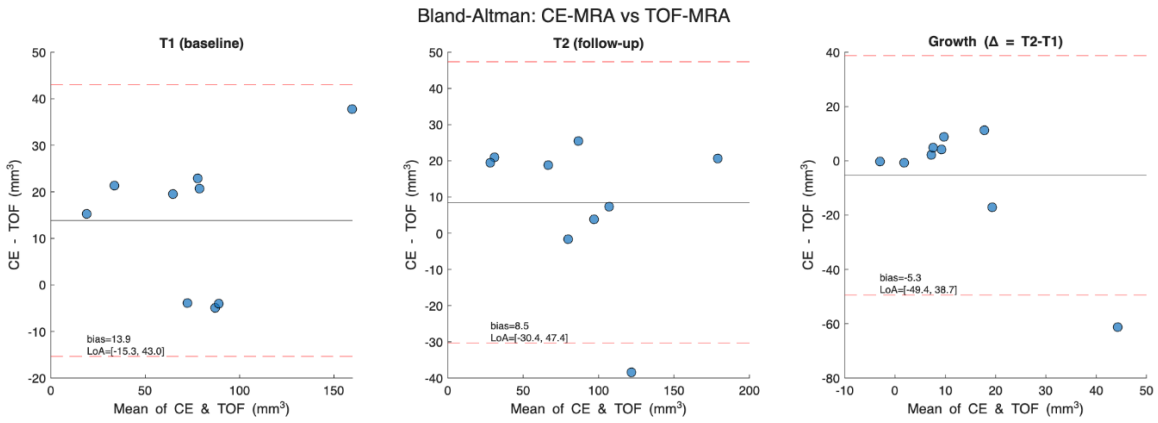

Figure 15. Bland-Altman Analysis
Bland-Altman Bias Graphical Analysis comparing CE-MRA and TOF-MRA for Timepoint 1, Timepoint 2, and Growth between Timepoint 1 and Timepoint 2.

Looking at the growth trends of the samples, it can be visually seen that between TOF-MRA and CE-MRA, the growth trajectories are qualitatively similar (Figure 16).

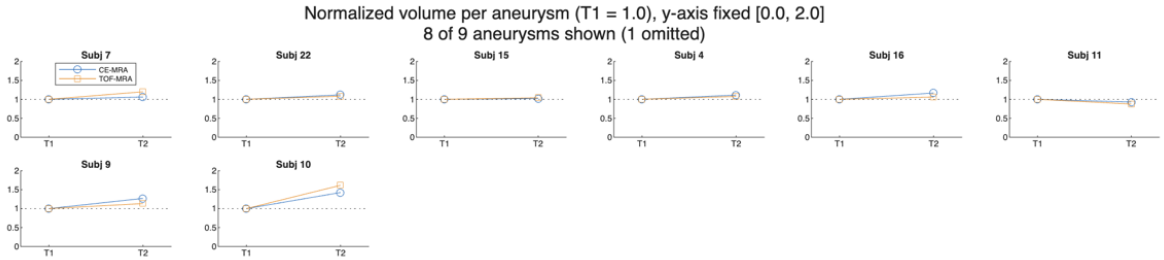

Figure 16. Growth Trajectories
Normalized Growth Trajectories for Individual Aneurysms (Ordered from Largest to Smallest)

When doing Wilcoxon Tests, results showed that CE-MRA for Timepoint 1 vs. Timepoint 2 had a median growth of 10.79 mm^3, and TOF-MRA for Timepoint 1 vs. Timepoint 2 had a median growth of 6.12 mm^3, showing that CE-MRA captured around 76.3% more growth when compared to TOF-MRA.

Similar to the size of aneurysms where larger aneurysms in TOF have significant saturation effects, when analyzing the proportional bias, the growth showed significant proportional bias with a

slope of -1.364, r of -0.834, and a p-value of 0.005 which showed that for the larger growth, TOF increasingly underestimates growth relative to CE.

The relative disagreement (in %) size between CE-MRA and TOF-MRA had an r of -0.639, a p-value of 0.0638, a mean relative agreement of 29.7%, and a median relative agreement of 26.3%.

Table 2: Summary of Statistics
Summary of the statistical analysis results that were run on the selected 9 aneurysms. Key values to note include the Pearson Correlation, which shows that at individual time-points both modalities had strong agreement of the overall aneurysm volume, but the correlation dropped when looking at the agreement regarding aneurysm growth. This finding was further supported by the ICC Agreement. The Bland-Altman Analysis highlighted the systematic bias of TOF-MRA volume being reported as lower than CE-MRA. The Wilcox Signed Rank Test showed that both modalities for aneurysms smaller than 6 mm successfully detected a change over time.

Test / Metric	T1 (Baseline)	T2 (Follow-up)	Growth (ΔVol)
Pearson Correlation — CE vs TOF			
r	0.935	0.919	0.344
p-value	0.0002	0.0005	0.3649
n	9	9	9
ICC(2,1) Agreement			
ICC	0.886	0.907	0.207
Interpretation	Good	Excellent	Poor
Bland-Altman Analysis			
Bias (mm^3)	+13.9	+8.5	−5.3
Limits of agreement	[−15.3, 43.0]	[−30.4, 47.4]	[−49.4, 38.7]
LoA span (mm^3)	~58	~78	~88
Wilcoxon Signed-Rank Tests			
CE vs TOF (p)	0.0547	0.1641	0.8203

Test / Metric	T1 (Baseline)	T2 (Follow-up)	Growth (ΔVol)
Time point 1 vs Time point 2 within modality (p)	CE: 0.0117 | TOF: 0.0117		
Median growth (mm^3)	CE: 10.79 | TOF: 6.12		
Proportional Bias (Difference vs Mean)			
Slope	0.096	−0.121	−1.364
r	0.256	−0.284	−0.834
p-value	0.5063	0.4595	0.0052
Disagreement Scaling Size			
Abs. disagreement vs size (r)	0.395 (p=0.293)		
Relative (%) disagreement vs size (r)	−0.639 (p=0.064)		
Mean / median relative disagreement	29.7% / 26.3%		

Discussion

One of the important findings of this study was identifying the difficulty in tracking a category of studies, in this case cerebral aneurysms, from a clinical database where the specific condition is not accurately specified and consistent imaging approaches are not specified or used. A second important finding was that TOF-MRA methods are poorly suited when aneurysm size is of the order of 6mm or greater, when flow saturation effects degrade the ability to meaningfully contour the aneurysm. Additionally, it was found that CE-MRA could also fail, but at a much lower rate than for TOF-MRA, concluding that it is a preferable approach for monitoring cerebral aneurysms over time.

Many of the imaging analysis issues from the TOF-MRA data stemmed from the tradeoff of minimizing noise through increased thresholds, which led to decreased aneurysm size and incomplete

delineation of the aneurysm. In the case of Aneurysm #1, Aneurysm #7, and Aneurysm #9, the incomplete signal saturation meant that volume growths that were visualized on the graphs were not reliable. Specifically for TOF-MRA images, because of the slow-flow effects and lack of a uniform higher steady-state signal intensity range compared to CE-MRA, when using the automated pipeline, even an arguably small change in the threshold meant changes in how the aneurysm of interest would be segmented.

A closer analysis of Aneurysm #4 indicates that along with magnetization saturation, image concerns may also stem from the presence of thrombus which mimics magnetization saturation. This was validated through the Black Blood Imaging acquisition (Figure 7). As seen in Figure 5, there is visible local growth observed at the top of the aneurysm. However, when looking at Figure 6, both CE-MRA and TOF-MRA show a decrease in aneurysm volume over time, which can be explained by the layering of thrombus (in CE-MRA specifically) or both the presence of thrombus and incomplete vessel volume filling (in TOF-MRA). This further highlights the lack of robustness and the difficulty of analyzing TOF-MRA image data due to the compounding effects of both thrombus presence and incomplete vessel volume filling (saturation effects).

Taking into consideration the issue identified with the CE-MRA imaging of Aneurysm #6, namely the artifact present in CE-MRA but not TOF-MRA, the measurements from the CE-MRA in this case would not be reliable and present one of the limitations of using CE-MRA for analysis. Because of this artifact, segmenting and clipping the aneurysm solely proved to be a limitation of the pipeline. Specifically addressing this, a future direction to explore is the incorporation of the Parent Vessel Reconstruction Methodology into our pipeline, allowing us to be more sensitive to the aneurysm volume changes, especially in the cases of small aneurysms. While this method uses the centerline information to estimate the parent vessel's curvature, it must be noted that there is a component of assumption that would be made to discriminate between parent vessel volume and aneurysm volume.

Considering the statistical analysis results, it can be noted that while the correlation values at Timepoint 1 and Timepoint 2 show that CE and TOF-MRA have strong agreement on volumes at the

individual timepoints, it only supports the idea that the two methods rank aneurysms similarly by size, but they do not reliably agree on how much an aneurysm has grown. With the TOF-MRA modality systematically underestimating the volume compared to CE which may be attributed to the saturation effects, using TOF data on aneurysms that are larger than 6 mm may not yield reliable and accurate results when monitoring growth on individual patients. The Wilcoxon Tests showed that the CE-MRA modality captured roughly 76.3% more growth than TOF-MRA which supports the notion that using TOF when monitoring growth in a clinical setting may underestimate growth rate and have different clinical implications. The proportional bias analysis also indicated that for larger growth values, TOF increasingly underestimated the growth when compared to CE-MRA. In other words, TOF performed worse than CE in cases of faster-growing and higher-risk aneurysms. The mean relative disagreement of 29.7% and a significant p-value of 0.064 suggests that smaller aneurysms have proportionally greater disagreement of the overall volume between the methods but have comparable trends of change over timepoints. However, all these analyses were done on a small sample set of 9 aneurysms, and thus, a much larger dataset of comparable TOF and CE-MRA scans would be needed to make more definitive and conclusive remarks.

As identified in the power analysis, we expect that increasing the sample size to include 22 or more TOF-MRA studies would permit us to make statistically meaningful conclusions. Along with increasing the analysis sample size, future directions to address other issues that arose include the possibility of incorporating a smoothing stage for the scans during processing to help discount the differences that may be due to the underfilled vessel volumes (namely in TOF-MRA). While more subjects need to be sampled before statistical analysis, such as obtaining the coefficient of variance, can be done, it must be noted that the TOF-MRA volumes consistently started at lower volumes for the first timepoint when contrasted against the CE-MRA, which may be indicative of increased variance. However, this may also be a side effect of the underfilling seen in TOF-MRA, leading to quantitatively “lower” starting volumes.

Taking the pipeline, especially regarding the issues of underfilling, there is a great value in exploring the possibility of changing the pipeline thresholding to better optimize it to the TOF-MRA data, which has a very different dynamic range of signals compared to CE-MRA. Initial investigations of the edge cases showed that there was no threshold that was low enough to accurately separate the aneurysm from the background, but as more samples are analyzed, this may change.

Compiling all the results, the visually poor quality of the TOF-MRA further highlights the importance of using CE-MRA to train a Deep /Machine Learning model to segment and perform volumetric analysis on TOF-MRA. As another potential future direction, this use case would need to be further studied for added value.

Conclusion

Based on this dataset, it is shown that TOF-MRA has more inherent image quality problems that drastically affect the reliability and validity of aneurysm volumetric analysis compared to CE-MRA. Further studies need to be conducted with a larger sample size to see whether the statistical findings are supported on a larger dataset; however, preliminary statistical analysis findings show that CE and TOF agree reasonably on size at a single timepoint, but do not reliably agree on the amount of growth. TOF underestimates growth magnitude and shows a proportional bias specifically in cases of larger growth. Moreover, looking at the failure rate of TOF-MRA compared to CE-MRA sheds light on the possibility of using CE-MRA for routine clinical use to get more reliable information on rupture risk. In summary, while TOF-MRA seems to reliably work on aneurysms that are less than 6 mm in size, it cannot be used as a reliable imaging modality on aneurysms that are larger than 6 mm in size and rather, CE-MRA should be used for routine clinical checks.

References

Anzalone N, Scomazzoni F, Cirillo M, Righi C, Simionato F, Cadioli M, Iadanza A, Kirchin MA, Scotti G. Follow-up of coiled cerebral aneurysms at 3T: comparison of 3D time-of-flight MR angiography and contrast-enhanced MR angiography. AJNR Am J Neuroradiol. 2008 Sep;29(8):1530-6. doi: 10.3174/ajnr.A1166. Epub 2008 Jun 12. PMID: 18556359; PMCID: PMC8119060.

Cirillo M, Scomazzoni F, Cirillo L, Cadioli M, Simionato F, Iadanza A, Kirchin M, Righi C, Anzalone N. Comparison of 3D TOF-MRA and 3D CE-MRA at 3T for imaging of intracranial aneurysms. Eur J Radiol. 2013 Dec;82(12):e853-9. doi: 10.1016/j.ejrad.2013.08.052. Epub 2013 Sep 12. PMID: 24103356.

de Nys, C.M., Liang, E.S., Prior, M. *et al.* Time-of-Flight MRA of Intracranial Aneurysms with Interval Surveillance, Clinical Segmentation and Annotations. *Sci Data* **11**, 555 (2024). https://doi.org/10.1038/s41597-024-03397-8

Liu X, Haraldsson H, Wang Y, Kao E, Ballweber M, Martin AJ, McCulloch CE, Faraji F, Saloner D; UCSF Intracranial Aneurysm Monitoring Group. A Volumetric Metric for Monitoring Intracranial Aneurysms: Repeatability and Growth Criteria in a Longitudinal MR Imaging Study. AJNR Am J Neuroradiol. 2021 Sep;42(9):1591-1597. doi: 10.3174/ajnr.A7190. Epub 2021 Jun 24. PMID: 34167960; PMCID: PMC8423054.

Maki JH, Chenevert TL, Prince MR. Contrast-enhanced MR angiography. Abdom Imaging. 1998 Sep-Oct;23(5):469-84. doi: 10.1007/s002619900384. PMID: 9841060.

Raghuram A, Patel R, Varon A, Sabotin R, Sanchez S, Derdeyn CP, Jabbour P, Hasan DM, Samaniego EA. Volumetric surveillance of brain aneurysms: Pitfalls of MRA. Interv Neuroradiol. 2023 Oct;29(5):532-539. doi: 10.1177/15910199221100619. Epub 2022 May 12. PMID: 35549745; PMCID: PMC10549707.

Sammy Allaw, Kameel Khabaz, Tyler C. Given, Dominic Montas, Roberto J. Alcazar-Felix, Abhinav Srinath, Tareq Kass-Hout, Timothy J. Carroll, Michael C. Hurley, Sean P. Polster A Review of Intracranial Aneurysm Imaging Modalities, from CT to State-of-the-Art MR American Journal of Neuroradiology Jun 2025, 46 (6) 1082-1092; DOI: 10.3174/ajnr.A8549

Śliwczyński A, Jewczak M, Dorobek M, Furlepa K, Gołębiak I, Skibińska E, Sarzyńska-Długosz I. An Analysis of the Incidence and Cost of Intracranial Aneurysm and Subarachnoid Haemorrhage Treatment between 2013 and 2021. Int J Environ Res Public Health. 2023 Feb 21;20(5):3828. doi: 10.3390/ijerph20053828. PMID: 36900834; PMCID: PMC10001767.

van der Kamp LT, Rinkel GJE, Verbaan D, van den Berg R, Vandertop WP, Murayama Y, Ishibashi T, Lindgren A, Koivisto T, Teo M, St George J, Agid R, Radovanovic I, Moroi J, Igase K, van den Wijngaard IR, Rahi M, Rinne J, Kuhmonen J, Boogaarts HD, Wong GKC, Abrigo JM, Morita A, Shiokawa Y, Hackenberg KAM, Etminan N, van der Schaaf IC, Zuithoff NPA, Vergouwen MDI. Risk of Rupture After Intracranial Aneurysm Growth. JAMA Neurol. 2021 Oct 1;78(10):1228-1235. doi: 10.1001/jamaneurol.2021.2915. Erratum in: JAMA Neurol. 2022 Mar 1;79(3):312. doi: 10.1001/jamaneurol.2021.5146. PMID: 34459846; PMCID: PMC8406207.

Villablanca, J. P., Duckwiler, G. R., Jahan, R., Tateshima, S., Martin, N. A., Frazee, J., Gonzalez, N. R., Sayre, J., & Vinuela, F. V. (2013). Natural history of asymptomatic unruptured cerebral aneurysms evaluated at CT angiography: Growth and rupture incidence and correlation with epidemiologic risk factors. Radiology, *269*(1), 258–265; DOI: 10.1148/radiol.13121188

Zhu C, Wang X, Eisenmenger L, Tian B, Liu Q, Degnan A.J., Hess C, Saloner D, Lu J. Surveillance of Unruptured Intracranial Saccular Aneurysms Using Noncontrast 3D-Black-Blood MRI: Comparison of 3D-TOF and Contrast-Enhanced MRA with 3D-DSA American Journal of Neuroradiology Jun 2019, 40 (6) 960-966; DOI: 10.3174/ajnr.A6080

Publishing Agreement

It is the policy of the University to encourage open access and broad distribution of all theses, dissertations, and manuscripts. The Graduate Division will facilitate the distribution of UCSF theses, dissertations, and manuscripts to the UCSF Library for open access and distribution. UCSF will make such theses, dissertations, and manuscripts accessible to the public and will take reasonable steps to preserve these works in perpetuity.

I hereby grant the non-exclusive, perpetual right to The Regents of the University of California to reproduce, publicly display, distribute, preserve, and publish copies of my thesis, dissertation, or manuscript in any form or media, now existing or later derived, including access online for teaching, research, and public service purposes.

Signed by:
Siri Tantry
A8CC6650C0E14FF...
Author Signature

08/31/2026
Date